Journal of
Proteomics & Bioinformatics

Research Article   **Open Access**

Identification of Fat Storage-Inducing Transmembrane Proteins 1 and 2 as Putative Therapeutic Targets for Heart Failure by Integrated Analysis of Proteome and Transcriptome

Natsumi Nishihama[1]*, Yuki Abe[2], Kazuishi Kubota[3], Takahiro Nagayama[4], Takehiro Hirai[5], Kenjiro Ueda[6], Kenji Nakamaru[7], Tsuyoshi Hirata[3], Keiichi Fukuda[8], Ryuta Koishi[1] and Shinji Makino[8]

[1]Venture Science Laboratories, R&D Division, Daiichi Sankyo Co., Ltd., 1-2-58, Hiromachi, Shinagawa-ku, Tokyo 140-8710, Japan
[2]Biologics & Immuno-Oncology Laboratories, Oncology Function, R&D Division, Daiichi Sankyo Co., Ltd., 1-2-58, Hiromachi, Shinagawa-ku, Tokyo 140-8710, Japan
[3]Research Management Department, Daiichi Sankyo RD Novare Co., Ltd., 1-16-13, Kitakasai, Edogawa-ku, Tokyo 134-8630, Japan
[4]Rare Disease Laboratories, R&D Division, Daiichi Sankyo Co., Ltd., 1-2-58, Hiromachi, Shinagawa-ku, Tokyo 140-8710, Japan
[5]Clinical Development Department, Daiichi Sankyo RD Novare Co., Ltd., 1-16-13, Kitakasai, Edogawa-ku, Tokyo 134-8630, Japan
[6]Pain & Neuroscience Laboratories, R&D Division, Daiichi Sankyo Co., Ltd., 1-2-58, Hiromachi, Shinagawa-ku, Tokyo 140-8710, Japan
[7]Biomarker Department, Oncology Function, R&D Division, Daiichi Sankyo Co., Ltd., 1-2-58, Hiromachi, Shinagawa-ku, Tokyo 140-8710, Japan
[8]Department of Cardiology and Health Center, Keio University School of Medicine, Shinano-machi 35, Shinjuku-ku, Tokyo 160-8582, Japan

Abstract

Cardiovascular disease constitutes a major health burden globally, for which novel cardiotonic agents are still required. Cardiac failure is thought to be caused by dysfunctions of the sarcoplasmic/endoplasmic reticulum (SR/ER) in cardiomyocytes. Therefore, in this study, we searched for novel pharmaceutical targets in SR/ER. Tissue and organelle specific proteome profiling by liquid chromatography coupled with mass spectrometry after gel electrophoresis separation identified 3,638 proteins in heart and liver SR/ER samples from a mouse transverse aortic constriction (TAC) model (heart failure). We also analyzed the transcriptome of heart tissue from the TAC model (heart failure, hypertrophy) and a myocardial infarction model using microarrays to identify differentially expressed genes in the diseased heart. Several genes were chosen for further studies following the proteome and transcriptome analyses. Of these, fat storage-inducing transmembrane proteins 1 and 2 (FITM1 and FITM2) were highly expressed in mouse and human heart and skeletal muscle. We investigated the functions of FITM1 and FITM2 *in vitro* and confirmed that they mediated lipid droplet (LD) formation and directly bound to triglycerides. *FITM1* and/ or *FITM2* overexpression in cells altered the levels of Ero1-Lα and PDI, which are ER stress marker proteins that protect against heart failure and affect cellular metabolism. Together, these results indicate that FITM1 and FITM2 are expressed in heart tissue and that their modulated expression or function can change LD formation, ER function, and cellular metabolism in cells. Thus, FITM1 and FITM2 are good drug target candidates.

Abbreviations: ACTB: β-actin; ATP2A2: ATPase, Ca^{2+} Transporting, Cardiac Muscle, Slow Twitch 2; BiP (HSPA5/GPR78): Heat Shock Protein Family A (Hsp70) Member 5; CCDC47: Coiled-Coil Domain Containing 47; CCDC51: Coiled-Coil Domain Containing 51; CCDC90b: Coiled-Coil Domain Containing 90B; CE-TOFMS: Capillary Electrophoresis-Time of Flight Mass Spectrometry; CHOP (DDIT3): DNA Damage Inducible Transcript 3; COA3: Cytochrome C Oxidase Assembly Factor 3; DTT: Dithiothreitol; EDTA: Ethylene Diamine Tetraacetic Acid; ER: Endoplasmic Reticulum; Ero1-Lα: Endoplasmic Reticulum Oxidoreductase 1 Alpha; FAM210A: Family with Sequence Similarity 210 Member A; FITM1: Fat Storage-Inducing Transmembrane Protein 1; FITM2: Fat Storage-Inducing Transmembrane Protein 2; HF: Heart Failure; IRE1a (ERN1): Endoplasmic Reticulum to Nucleus Signaling 1; IVT: *In vitro* Transcription; LD: Lipid Droplet; LC-TOFMS: Liquid Chromatography-Time of Flight Mass Spectrometry; MI: Myocardial Infarction; MINOS1: Mitochondrial Inner Membrane Organizing System 1; MMgT1/Mmgt1: Membrane Magnesium Transporter 1; MO: Morpholino; MYC: Myelocytomatosis Oncogene; PDI: Protein Disulfide Isomerase; PBS: Phosphate-Buffered Saline; PERK: PRKR-like Endoplasmic Reticulum Kinase; Ppia: Peptidylprolyl Isomerase A; qPCR: Quantitative Polymerase Chain Reaction; RyR: Ryanodine Receptor; SLC12A4: Solute Carrier Family 12 Member 4; SLC25A35: Solute Carrier Family 25 Member 35; SR: Sarcoplasmic Reticulum; TAC: Transverse Aortic Constriction; Tbp: TATA-Box Binding Protein; TIMM21: Translocase of Inner Mitochondrial Membrane 21; Tmem38A: Transmembrane Protein 38A; Tmem38B: Transmembrane Protein 38B; Tmem242: Transmembrane Protein 242; UPR: Unfolded Protein Response.

Introduction

Heart failure (HF) is a condition in which the heart is unable to pump sufficiently to keep blood flow for transferring an enough amount of blood to the tissues. At least 1%–2% of people worldwide are affected by HF. The prevalence of HF is predicted to increase with the aging of global societies, which will have a major impact on healthcare systems [1-3]. The use of β-blockers and angiotensin-converting-enzyme inhibitors prolongs the survival time of HF patients, but their prognosis remains poor and HF-related mortality remains high. In 2015,

angiotensin II receptor blocker, neprilysin inhibitor, and funny (I*f*) channel inhibitor were all approved for clinical use globally, which have improved HF outcomes regarding cardiac mortality and hospitalization [4,5]. However, no treatment that targets the mechanisms of HF is available. The discovery of useful therapeutic drug targets for HF would therefore be very advantageous. The heart consists of different cell types, such as smooth muscle cells, pacemaker cells, endothelial cells, epicardial cells, cardiac fibroblasts, and cardiomyocytes [6]. Among these cells, dysfunctions of cardiomyocytes cause HF, likely due to the reduction of sarcoplasmic reticulum (SR) function. SR and endoplasmic reticulum (ER) are intracellular organelles that regulate calcium homeostasis, triglyceride synthesis, and protein folding [7-10]. SR has been well studied in cardiomyocytes. It stores calcium ions (Ca^{2+}) in these cells, which are located near the myofilaments and which regulate excitation–contraction coupling [11,12]. In a failing heart, smaller and slower contractions and smaller and less extensive relaxations in cardiomyocytes have been reported [13-15]. These dysfunctions are caused by the impairment of Ca^{2+} release and removal from SR. Thus, targeting of the SR could improve both systolic and diastolic functions of diseased hearts. It was recently, proposed that functions of the ER are also involved in the pathogenesis of HF [16,17]. ER is a site of the synthesis of membrane and secreted proteins, protein folding, lipid synthesis, and regulation of calcium homeostasis in various cell types [18-21]. Disruption of ER function induces the accumulation of unfolded proteins. The sensing of the accumulation activates defensive signaling in this organelle, which is termed the ER stress response/unfolded protein response (UPR). The UPR is initially adaptive for stress. However, if accumulation of unfolded proteins in cells continues, cell death can occur. UPR-related gene expression is increased in cardiac hypertrophy, HF, and myocardial infarction in human and animal models [16,17,22-28]. These findings suggest that the modulation of ER stress and ER-associated pathways may lessen the effects of HF. With this background, we explored novel pharmaceutical targets in SR/ER by proteomic and genomic approaches, and fat storage inducing transmembrane protein 1 and 2 (FITM1 and FITM2) were identified as candidates. Prior research has shown that FITM1 or FITM2 each have six-transmembrane domains and participate in lipid droplet (LD) formation [29-31]. However, their cardiac functions are not fully understood. Here, we report the expression profiles of FITM1 and FITM2 in mouse and human, their functions *in vitro*, and their effects on the cardiovascular system and body development in zebrafish. The findings show that FITM1 and FITM2 influence LD formation, ER stress response-related gene expression, and cellular metabolism *in vitro*, suggesting their potential to modulate HF pathogenesis.

Materials and Methods

Animal models

Seven-week-old male C57Bl/6 mice were purchased from Japan SLC, Inc. The mice were kept in a room at 55% relative humidity (permissible range: 30%–70%) and 23°C (permissible range: 20–26°C) under a 12 h light/dark cycle. At 9 weeks of age, the mice were intubated and anesthetized with isoflurane gas. To generate a chronic HF model induced by pressure overload, the transverse aorta was exposed by median incision, and pressure overload was conducted by transverse aortic constriction (TAC) using a 27-gauge needle. To generate a chronic HF model induced by myocardial infarction (MI), the chest cavity was exposed by cutting the intercostal muscle and the left coronary artery was ligated with 7-0 silk suture. Sham-operated control mice for each model underwent the same surgical procedure but without aortic constriction or coronary artery ligation. The animal

experiments were carried out in accordance with the guidelines of the local Institutional Animal Care and Use Committee.

Left Ventricle (LV) sample collection

At 4–5 weeks after surgery, cardiac functions were assessed by transthoracic echocardiography in conscious mice using an Aplio SSA-770A device (Toshiba Medical Systems Corporation, Japan) equipped with a 15-MHz linear-array transducer. Mice diagnosed with HF by echocardiography were sacrificed and the LV was excised. Messenger RNA (mRNA) and protein were isolated from the LV tissues frozen in liquid nitrogen. Expression of mRNA and protein was assessed using standard techniques.

Preparation of SR and ER

SR and ER from heart and liver tissue were prepared using the Endoplasmic Reticulum Enrichment Kit (Novus Biologicals, USA) following the manufacturer's protocol. LVs were collected from mice 4–5 weeks after TAC manipulation and from control mice. The tissues were washed in 10 ml of phosphate-buffered saline (PBS), cut into small pieces, and homogenized in isosmotic homogenization buffer containing protein inhibitor cocktail. Liver tissue was also homogenized to prepare the ER fraction and to identify SR-specific proteins. A mixture of homogenized tissues (0.5 g) from three mice was centrifuged at $1,000 \times g$ for 10 min at 4°C. The obtained supernatant was centrifuged at $12,000 \times g$ for 15 min at 4°C. The supernatant obtained from this procedure was centrifuged at $90,000 \times g$ for 60 min and the pellet was dissolved in PBS and used as the SR fraction. Liver tissue samples were subjected to the same procedure to prepare the ER fraction.

Protein identification by Mass Spectrometry (MS)

Twenty micrograms of proteins were separated on to sodium dodecyl sulfate-polyacrylamide gel electrophoresis gel (SDS-PAGE) and stained with Coomassie brilliant blue staining. The gel was sliced into 12 pieces from the dye front to the top of the gel. Each slice was minced and destained at 30°C for 30 min using 20 mM NH_4HCO_3 (pH 8) containing 50% acetonitrile. Digested samples were dehydrated with acetonitrile and dried by a centrifugal evaporator. The dried gel samples were rehydrated with a buffer (100 mM NH_4HCO_3, pH 8, containing 6 M guanidine-HCl, 10 mM ethylenediaminetetraacetic acid (EDTA), and 10 mM dithiothreitol (DTT)), and the total protein in the gels was reduced at 95°C for 5 min. The gel samples were cooled to 20°C and immersed in 100 mM NH_4HCO_3 (pH 8) containing 6 M guanidine-HCl, 10 mM EDTA, and 50 mM iodoacetamide. The proteins in the gel slices were dehydrated with acetonitrile and dried using a centrifugal evaporator. The dried gel slices were rehydrated in 20 mM NH_4HCO_3 (pH 8) containing 0.005% n-dodecyl-β-D-maltopyranoside (DM; Nacalai Tesque, Japan) and 5 ng/μl modified trypsin (Promega, USA). Proteins were digested at 37°C for 12 h and the resulting peptides were extracted once with FA/H_2O buffer (0.05% formic acid containing 0.005% DM) and twice with FA/ACN buffer (0.05% formic acid in acetonitrile) for 5 min each. The collected extracts were then concentrated to approximately 20 μl by an evaporator and analyzed by liquid chromatography tandem mass spectrometry (LC-MS/MS). Samples were desalted and concentrated using StageTips [32] by a slightly modified version of the previously reported protocol. First, a blunt-tipped hypodermic needle was manually pushed through an Empore Disk C18 (3M, USA) similar to the action of a cookie cutter. The two cut disks were inserted into the tip of a model P200 pipette (Rainin, USA). All solutions were loaded

from the top of the tip using a pipette. The liquid was pressed through the tip and centrifuged at 3,500 × g. The StageTip was first activated by 20 μl of methanol and conditioned using 20 μl of 5% formic acid containing 50% acetonitrile, and then equilibrated with 20 μl of 5% formic acid. After sample loading, the tip was washed with 20 μl of 5% formic acid and the desalted peptides were eluted from the tip with 40 μl of 5% formic acid containing 50% acetonitrile. An LTQ-Orbitrap or LTQ-Orbitrap XL (both from Thermo Fisher Scientific, USA) was equipped with a model 1100 liquid chromatography system (Agilent Technologies, USA) modified with an in-house flow splitter to produce a flow rate of 200–300 nl/min. A custom-made electrospray ionization tip column (100 μm internal diameter, 150 mm in length) was packed with Inertsil ODS-3 C18 (3 μm; GL Sciences, Japan). The elution of peptides was carried out with a linear gradient of 5%–28% acetonitrile over 100 min. Each sample volume was 4 μl and all measurements were made in duplicate. The MS/MS data were searched against the IPI mouse Mascot database (Matrix Sciences, USA) and filtered with a false discovery rate of 1% at the protein level by a target-decoy approach [33]. Proteins were quantified by Mascot score. In case higher Mascot score of protein was more than 1000, more than 3-fold difference of Mascot score between comparison was regarded as up- or down-regulated. In case higher Mascot score was more than 100, more than 5-fold difference was regarded as up- or down-regulated. Otherwise, 10-fold difference was needed for up- or down-regulated proteins.

Gene annotation

A membrane protein, transporter, ion channel, and calcium binding protein annotated in the Gene Ontology database (http://www.geneontology.org/) were selected as membrane proteins from the list of the proteins identified by MS. In addition, proteins with a membrane domain predicted by SOSUI software (http://bp.nuap.nagoya-u.ac.jp/sosui/) or TMHMM software (http://www.cbs.dtu.dk/services/TMHMM/) were also selected. The expression of all target genes in the heart was assessed by using the BioExpress database (GeneLogic, USA).

Total RNA isolation and microarray analysis

For the MI model, LV of three sham mice and four MI mice were used. For the TAC model, LVs of three sham mice, three HF mice, and three heart hypertrophy mice were used. Total RNA was isolated from tissues using TRIzol reagent (ThermoScientific, USA) and was purified with an RNeasy Mini Kit (Qiagen, Germany) following the manufacturer's instructions. Total RNA yields were quantified with a NanoDrop ND-8000 spectrophotometer (ThermoScientific, USA) and the RNA quality was assessed on RNA 6000 NanoChips with the 2100 Bioanalyzer (Agilent Technologies, USA). Microarray processing was conducted according to the GeneChip Expression Analysis Technical Manual (Affymetrix, USA). Arrays were scanned using GeneChip Scanner 3000 7G (Affymetrix, USA). The scanned images were processed using the Affymetrix GeneChip Command Console software to generate CEL files. In vitro transcription (IVT) reaction and hybridization quality were assessed with the Expression Console software (Affymetrix, USA). Normalized expression signals were calculated from CEL files using the MAS5 algorithm normalization method and the mean value of all signals, except the top 2% and the bottom 2%, was adjusted to 150.

Plasmid constructs

FITM1 and FITM2 plasmid constructs (the backbone vector is pCMV6) were obtained from OriGene (USA).

Cells

Human embryonic kidney (HEK)293 cells were maintained in Dulbecco's Modified Eagle Medium, High Glucose, Pyruvate (Life Technologies, USA) supplemented with 10% fetal bovine serum at 37°C in an atmosphere of 5% CO_2. For the overexpression of FITM1 and/or FITM2, constructs were transfected using Lipofectamine 2000 reagent (Life Technologies, USA) in accordance with the manufacturer's protocol.

Microscopy

Transfected cells were fixed with 10% Formalin Neutral Buffer Solution (Wako, Japan). Cells were stained for LDs using 1 μg/ml BODIPY 493/503 (Life Technologies, USA) for 5 min at 37°C and 5% CO_2, and for nuclei using 2.5 μg/ml Hoechst 33342 (Life Technologies, USA) for 25 min at room temperature. Samples were washed twice with PBS and analyzed using an EVOS microscope (Life Technologies, USA) equipped with a 40× lens at room temperature and using an IN Cell Analyzer 1000 (GE Healthcare, USA) to measure the number and size of LDs with a 20× lens at room temperature.

Lipid binding assays

Recombinant FITM1-His6-StrepII and FITM2-His6-StrepII were generated by a previously described method [30]. Recombinant baculoviruses were constructed in pIEX-Bac1 expression vector (EMD Biosciences, USA) and recombinant proteins were overexpressed in Hi5 insect cells. Recombinant proteins were purified from the cells by sonication using Strep-Tactin Superflow Plus (Qiagen, Germany) and HiLoad16/60 Superdex75 (GE Healthcare, USA). Samples were suspended in storage buffer comprised of 50 mM Tris-HCl (pH 7.4), 150 mM NaCl, 10% glycerol, and 0.1% (w/v) Fos-Choine13 (Anatrace, USA). Binding of recombinant FITM1-His6-StrepII and FITM2-His6-StrepII to [9, 10^{-3}H(N)]-triolein was measured using a previously reported method [30] using three buffers. Buffer 1 comprised 50 mM Tris-HCl pH 7.4, 150 mM NaCl, and 0.1% (w/v) Fos-choline13. Buffer 2 comprised 50 mM Tris-HCl (pH 7.4), 150 mM NaCl. Buffer 3 comprised 10 mM Tris-HCl (pH 7.4), 150 mM NaCl, 1 mM EDTA, and 1% (w/v) Triton X-100. Each reaction was performed in 100 μl of Buffer 1 containing recombinant FITM1-His6-StrepII or FITM2-His6-StrepII, which was diluted in Buffer 1, 50 nM to 1 μM [9, 10^{-3}H(N)]-triolein in Buffer 2, and 15–30 μl of Strep-tactin Macroprep (IBA GmbH, Germany), which had been prewashed and suspended in Buffer 1. The reaction mix was subjected to inversion mixing for 4 h at room temperature and then mixed by vortexing at a power level of five to six after incubation. After the reaction, Strep-tactin Macroprep beads were washed three times with Buffer 1 and once with Buffer 3 by centrifugation and then re-suspended in 500 μl of Buffer 3. The suspension was then added to 10 ml of Hionic Fluor (PerkinElmer, USA) and the retained radioactivity was measured using a scintillation counter.

Western blotting

Cells were lysed in Laemmli sample buffer (Bio-Rad, USA) with 2-mercaptoethanol by sonication and boiled for 5 min at 95°C. Samples were run on 10%–20% Perfect NT gel (DRC, Japan) and transferred to polyvinylidene fluoride membranes (Merck Millipore, USA). Measurement of ER stress marker proteins was conducted using the ER Stress Antibody Sampler Kit (Cell Signaling Technology, USA) in accordance with the manufacturer's manual. Anti-myc antibody was used to confirm transfection and β-actin was used as a control. Bands were detected in a second reaction using horseradish peroxidase-conjugated anti-rabbit IgG or anti-mouse IgG antibody (GE Healthcare,

USA), ECL Prime Western Blotting Detection Reagent (GE Healthcare, USA), and LAS-3000 (Fujifilm, Japan).

Metabolomics

For pretreatment, culture of 1×10^6 cells per plate was performed. The culture medium was removed from the plates and 10 ml of 5% mannitol solution was added to wash the cells. After washing the cells, 1,300 μl of methanol containing 10 μM of commercial Internal Standard Solution 1 (Solution ID: H3304-1002; Human Metabolome Technologies, Japan) was added. Cells were scraped from the plate and 1,000 μl of cell lysate was used. Half of the cell lysate volume was used for capillary electrophoresis-time of flight mass spectrometry (CE-TOFMS) measurement. Two hundred microliters of Milli-Q water and 500 μl of chloroform were added to the samples, mixed, and centrifuged at 2,300 × g at 4°C for 5 min. Proteins in 400 μl of upper aqueous phase were removed using a Millipore 5-kDa cutoff filter. The filtered samples were lyophilized and suspended in 50 μL of Milli-Q water, and analyzed by CE-TOFMS. The remaining 500 μl of the cell lysate suspension was used for liquid chromatography (LC)-TOFMS measurement. Samples were ultrasonically agitated for 5 min, and then centrifuged at 2,300 × g at 4ºC for 5 min. Supernatant was lyophilized and suspended in 100 μl of a 1:1 mix of isopropanol and Milli-Q water, and analyzed by LC-TOFMS. Metabolome measurements were carried out at Human Metabolome Technologies Inc.

Quantitative analysis of mRNA expression levels

Gene expression analysis was conducted by quantitative polymerase chain reaction (qPCR) using the Taqman system (Applied Biosystems, USA). Commercial cDNAs (Clontech, USA, Biochain, USA) were used for the analysis. Relative mRNA levels were quantified with the comparative ΔΔCT method using an internal control gene. The primers used were:

FITM1: Hs00416856_g1 / Mm01322192_g1

FITM2: Hs00380930_m1 / Mm04212060_m1

TIMM21 (1700034H14Rik / C18orf55): Hs01003272_g1

FAM210A (4933403F05Rik / C18orf19): Hs00935911_m1

SLC12A4: Hs00957115_g1

TMEM242 (5730437N04Rik / C6orf35): Hs00218395_m1

Internal control

Tbp: Mm00446971_m1

Ppia: 4326316E / Mm02342429_g1

β-Actin: 4333762F

Fish husbandry

RIKEN WT zebrafish were raised and maintained in accordance with standard protocols [34]. Embryos were collected after natural spawning and maintained at 28°C.

Morpholino (MO) gene knockdown in zebrafish

MOs bind to and block the translation of mRNA *in vivo*. The MOs we used (GeneTools, USA) were re-suspended in sterile water and diluted to the chosen concentrations ranging from 10–500 μM. Approximately 1 nl was injected using a microinjector (Narishige, Japan) into embryos at the one-cell stage. Effective doses were separately determined for each MO. Penetrance numbers using morphological criteria were

verified independently in comparison to control-injected samples, in each example using a specific concentration. Minimum sample sizes of 50 were used in each case. The MOs used were:

MO-control	5'-TTTCCAAATTTTGATACGTACGATG-3'
FITM1	5'-CCACAAGGATCGAGTTTAGAAACAT-3'
FITM1-5mis	5'-CCAGAACGATGGACTTTACAAACAT-3'
FITM2	5'-TGCAACGGCAGCAGCCATGTTGTTC-3'
MMgT1	5'-CACCTTTCCAGAAGGACGAGGCCAT-3'
MMgT1-5mis	5'-CACGTTTGCACAAGCACCAGGCCAT-3'

Timm21 (1700034H14Rik)
5'-ATGTCTTGTCGTTTAACCAACACAC-3'

Ccdc51	5'-CAGTGTTTGTTCTGAACCTCATTGA-3'
Ccdc51-5mis	5'-CACTCTTTCTTCTCAACCTCATTCA-3'

Fam210a (4933403F05Rik)
5'-TCCAGAACACACAAACCGCTGCATC-3'

Fam210a-5mis	5'-TCGACAACAGACAAAGCCCTGCATC-3'
Tmem38a	5'-AGGACATCTAACACCTCCATGATGT-3'
Tmem38b	5'-AACACATCCATAACTGAGCCGCTTC-3'

Minos1 (2310028O11Rik)
5'-GCTCTTTCTCAGACATGATGACAGC-3'

Ccdc90b	5'-GTCTCCGCATAAAGATCCCCCAGGA-3'
Slc12a4	5'-TTTCATGTGTTTAGTGTGCGGATCA-3'
Coa3 (Ccdc56)	5'-TACTCATGTCTGCCATGTTTGAGGC-3'
Slc25a35	5'-CGACGCCACCGAGAATGAAATCCAT-3'
Tmem65	5'-CAGCAACACCGAGCGGATCATCAGA-3'

Tmem242 (5730437N04Rik)
5'-GCTCTACTGACATCTGAATAGGTC-3'

mRNA injection

Each open reading frame of FITM1 or FITM2 was amplified by PCR from IMAGE clones obtained from Open Biosystems (USA). Respective PCR products were purified and sub-cloned into pCS2⁺ [35]. Recombinant clones were linearized by the digestion with NotI and the capped mRNA was synthesized *in vitro* using the mMESSAGE mMACHINE kit (Ambion, USA). Synthetic mRNA (0.8 μg/μl) was injected into Zebrafish embryos at the one-cell stage.

Statistical analyses

Differences were tested by two-tailed t-test. For transcriptome analysis, adjusted p-values were also calculated by R software using the Benjamini & Hochberg method [36] to control of the false discovery rate for multiple comparisons. For metabolome analysis, differences were tested by Welch's t-test. The p-values <0.05 were considered statistically significant. Data analysis was done using Excel 2010 software (Microsoft, USA).

Results

Proteome profile of mouse heart SR/ER

To identify proteins expressed in SR/ER of mouse heart, we first

attempted to obtain the proteome profile of heart and liver SR/ER fraction from a TAC model. The TAC model is the most commonly used pressure overload heart failure model in rodents, in which a fixed aortic constriction leads to the inhibition of cardiac flow as well as dilation of the LV with reduced ejection fraction [37]. We chose to apply LC-MS/MS with SDS-PAGE separation, which is termed GeLC-MS/MS, to ensure that the proteome profiling was as comprehensive as possible [38]. In total, we identified 3,638 proteins from three samples: healthy SR/ER, TAC SR/ER, and liver ER proteins (Figure 1 and Supplementary Table 1). There were 1,232 and 824 proteins specifically identified from heart and liver samples, respectively. We attempted to identify up- or down-regulated proteins in the TAC model. However, only 333 up-regulated and 163 down-regulated proteins were identified in this dataset, probably because overall protein expression changed little as a result of TAC. We provided all 1,232 identified proteins with annotations, such as gene symbol, number of predicted transmembrane regions, enzyme domain, and localization. In this list, genes reported to be expressed in SR, such as *Atp2a2* (*SERCA2a*), *Ryr2*, *Ccdc47* (*Calumin*) [39], and *Tmem38a (TRIC-A)* [40], were included, suggesting the good quality of this dataset.

Transcriptome analysis of mouse heart

We also tried to identify the genes that were expressed or exhibit a change of expression level in heart failure. We analyzed the heart from the TAC model (heart failure, hypertrophy) and an MI model by

Figure 1: Left panel: Procedure and result of the 1st experiment. The LV from TAC (HF) and healthy control (Ctrl) mice were excised and the SR/ER fractions were isolated. Proteins were electrophoretically separated and stained with Coomassie brilliant blue staining. The gel was sliced into 12 pieces from the dye front to the top of the gel. Each slice was analyzed by LC-MS/MS and identified 1,875 proteins. Right panel: Procedure and result of the 2nd experiment. In this trial, the LV and liver were used. 2,654 proteins were identified. In total, 3,638 proteins were identified by GeLC-MS/MS. We categorized these proteins by their expression pattern, such as; H (heart) >L (liver): proteins expressed in heart than liver, H=L: proteins which were expressed almost equally in heart and liver, H<L: proteins expressed in liver than heart.

microarray. MI is induced in the chronic heart failure model because of volume overload, in which MI induces hypertrophy with wall thinning [36]. The clustering results of the MI model data showed small individual differences. On the other hand, the clustering results of the TAC model data showed large differences between individuals in the hypertrophy group, so this group was excluded from the analysis. We compared gene expression data between the heart failure group and the sham group of the MI and TAC models to identify differentially expressed genes in heart failure. The percentages of the cells present in all experiments were roughly equal. The signal ratios of the 5'-probeset and 3'-probeset of β-actin and glyceraldehyde-3-phosphate dehydrogenase in all experiments were within the acceptable range. There was no problem about the quality of mRNA and cDNA of all samples. The ANP and BNP signals, which are biomarkers of heart failure, were higher in the heart failure group than in the sham group, and the Pearson's correlation coefficients among the intragroup samples were higher than among the intergroup samples. Therefore, we concluded that there was no misidentification of samples and no procedural error in the experiment. Those genes whose probeset showed a signal >50 and a valid value <0.05 in at least one sample in each model of MI or TAC were considered to be reliable genes (19,720 probesets for the MI model, 20,280 probesets for the TAC model, Supplementary Table 2). The genes whose probeset showed an average signal ratio of the sham group to the HF group in each model of MI or TAC of >1.5 or <0.667 with a difference (t-test, $p < 0.05$) were considered to be genes that were up- or down-regulated in heart failure (2,608 probesets for the MI model, 2,168 probesets for the TAC model). A total of 978 probesets were shared between the MI and TAC models (38% in the MI model, 45% in the TAC model).

Selection of putative pharmaceutical target genes

From the literature and information on the number of predicted transmembrane regions, enzyme domain, localization, and gene chip analysis, 22 genes were considered to encode functionally unknown membrane proteins that had homologs in zebrafish. To select candidates, we investigated the mRNA expression pattern in human tissues. Quantitative RT-PCR (qPCR) analysis indicated that five genes (*FITM1*, *TIMM21*, *FAM210A*, *TMEM242*, and *SLC12A4*) were highly expressed in skeletal muscle and/or heart (Figure 2). *Fitm2* is a member of the same family as *Fitm1*, but its protein was not detected in MS analysis in mouse samples, although it was detected in MS analysis using a human heart sample (data not shown). In addition, detection of Fitm2 protein in heart tissue by western blotting has been reported [29]. Therefore, we also evaluated the expression pattern of this gene. *Fitm2* was highly expressed in the heart (Figure 2). We also observed the effects of the 22 selected genes on cardiac functions using a zebrafish model. Zebrafish screening has advantages that include high throughput because of their prolific and fast growth, detection of phenotype by microscopy because the embryos are transparent, observation of cardiac dysfunctions as a systemic phenotype caused by abnormal distribution of yolk sac nutrients, and ability of cardiac mutant zebrafish to survive and continue to develop for several days. Knockdown of 11 genes, including *Fitm1*, was associated with cardiovascular dysfunction (Supplementary Figure S1). MO-mediated knockdown of *Fitm1* in zebrafish led to cardiovascular system dysfunctions that included cardiac edema and hypertrophy (Supplementary Figure S2a, 2b and Supplementary Table 3), but *Fitm2* knockout had no effect (Supplementary Figure S1). However, a double knockdown of *Fitm1* and *Fitm2* showed a more severe phenotype than the single knockdown of *Fitm1*, including no blood flow, cardiac edema, and a slow heartbeat (Supplementary Figure 2c, 2d and Supplementary
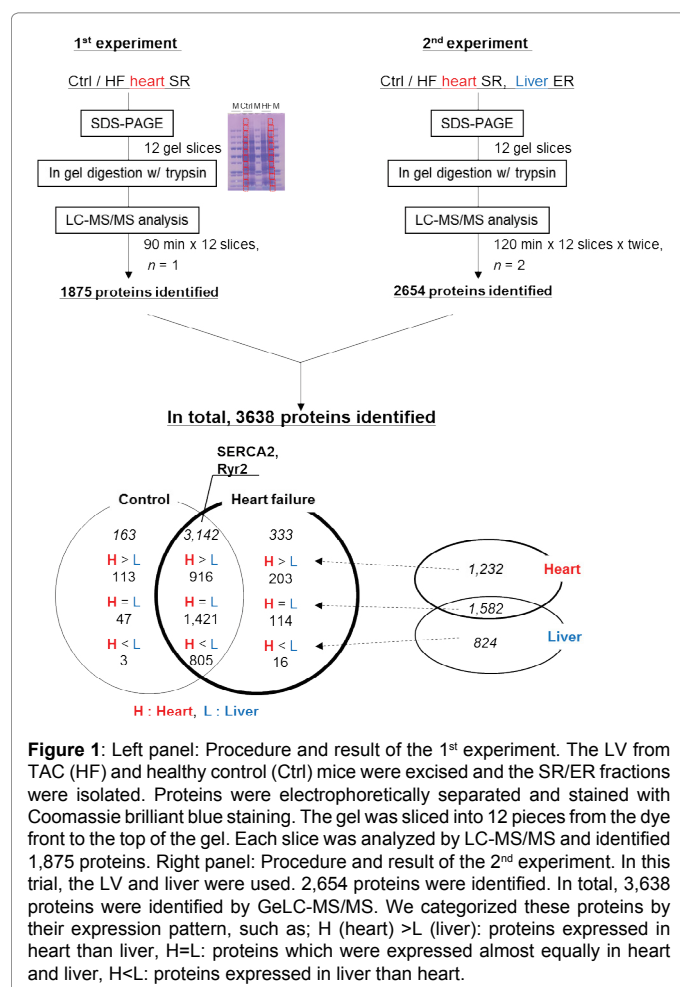
Table 4). Upon the injection of human *FITM1* or *FITM2* mRNA into zebrafish, skeletal malformation and cardiac edema were observed. The effect of *FITM2* mRNA injection was more severe than that of *FITM1* (Supplementary Figure 2e). Overall, six genes were highly expressed in heart and/or skeletal muscle, and showed phenotypic changes in zebrafish screening, and were regarded as putative targets (Table 1). In these six genes, even though their function in the heart was unknown,

FITM1 and *FITM2* were reportedly involved in LD formation [29,30,41]. Thus, we selected FITMs for further functional analysis.

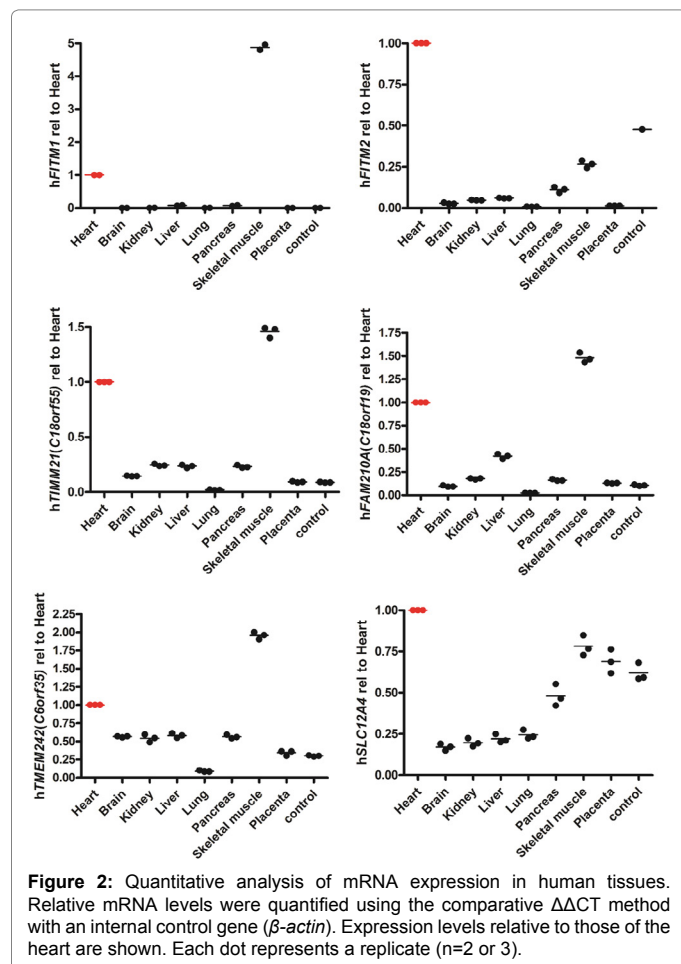### *FITM1* and *FITM2* are highly expressed in heart and skeletal muscle

As shown above, *FITM1* and *FITM2* were found to be highly expressed in heart and skeletal muscle in human tissues (Figure 2). qPCR analysis of mouse tissues also indicated their high expression in heart and skeletal muscle (Figure 3a). We next investigated their expression pattern in the different chambers of the human heart. *FITM1* and *FITM2* were highly expressed in the right ventricle (Figure 3b).

FITMs mediates lipid droplet formation *in vitro*

Next, we investigated the cellular function of FITMs to confirm their potential as drug targets. One of the cellular functions of FITM1 and FITM2 is in LD formation. We thus investigated LD accumulation using cells overexpressing these proteins. Upon the transient overexpression of *FITM1* and/or *FITM2* in HEK293 cells, LD accumulation was observed. *FITM2*-overexpressing cells produced larger and more LDs than *FITM1*-overexpressing cells (Figure 4a–g). In cells overexpressing both *FITM1* and *FITM2*, the number and size of LDs were intermediate between those produced upon *FITM1* or *FITM2* single transfection (Figure 4e–g). *FITM1* and *FITM2* were previously shown to be involved in LD formation by the direct binding of triglyceride [30], so we investigated this activity using recombinant proteins. Recombinant FITM1 and FITM2 bound [9, 10^{-3}H(N)]-triolein ([^{3}H]-TG) in a protein- or [^{3}H]-TG dose-dependent manner (Figure 5). These results were reproducible for three lots of recombinant protein.
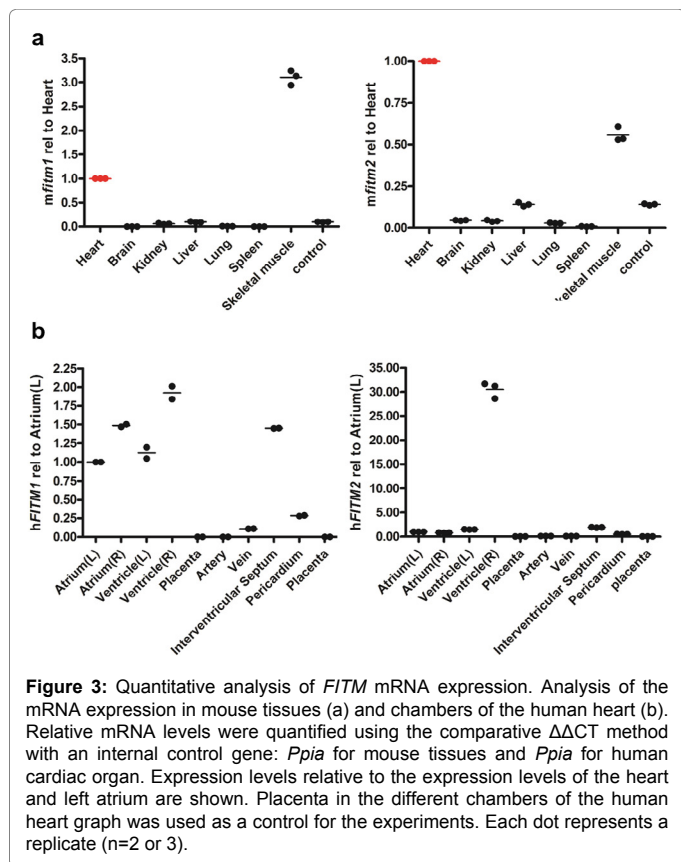
FITMs affect ER stress response and cellular metabolism

The results confirmed the function of FITMs in LD formation. However, little is known about how FITM1, FITM2, and LD are involved in heart function. Thus, we next investigated the effects of FITM1 and FITM2 on SR/ER function and cellular metabolism. The site where LDs initially form has not been definitively clarified, but it is widely thought to be at the ER membrane. We thus analyzed the change of the expression level of ER stress marker proteins in cells with accelerated LD formation by western blotting. In cells overexpressing FITMs, LDs accumulated and the expression levels of ER oxidoreductase 1 alpha (Ero1-Lα) and protein disulfide isomerase (PDI) were decreased

Figure 2: Quantitative analysis of mRNA expression in human tissues. Relative mRNA levels were quantified using the comparative ΔΔCT method with an internal control gene (*β-actin*). Expression levels relative to those of the heart are shown. Each dot represents a replicate (n=2 or 3).

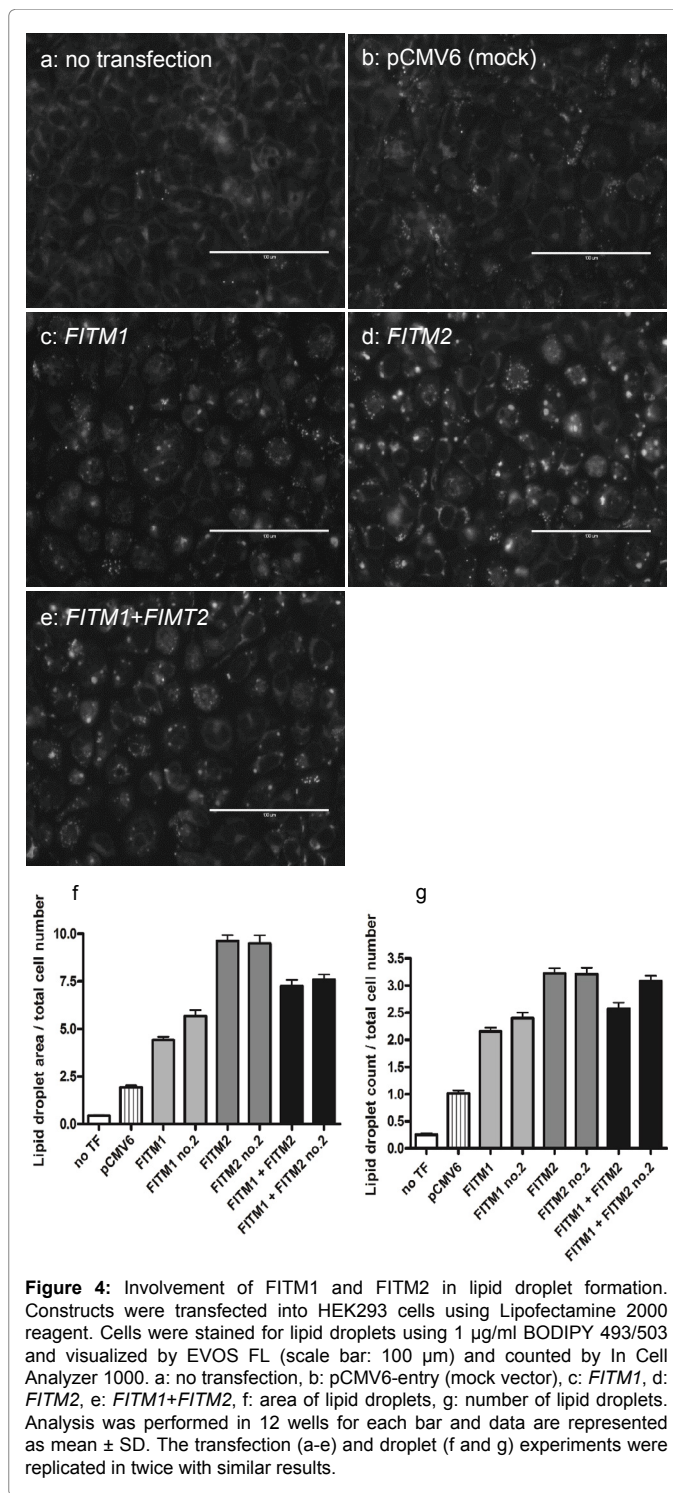| Symbol | Heart SR MS | Microarray | | | NCBI Accession # | Amino acids length & Transmembrane Prediction (TMHMM) | Cellular Localization (Prediction) |
	Mouse TAC *vs.* Normal	MI *vs.* Normal	TAC (heart failure) *vs.* Normal	TAC (hypertrophy) *vs.* Normal			
Fitm1	→	0.62	0.58	0.8	NP_081084	292 AA., 6TM	ER
Fitm2	-	0.63	0.63	0.77	NP_775573	262 AA., 6TM	ER
Timm21	→	0.82	0.85	0.9	NP_080245	244 AA., 1TM	Mit
Fam210a	→	0.66	0.8	0.84	NP_722489	273 AA., 1TM	Mit
Tmem242	→	0.89	0.83	0.97	NP_081733	140 AA., 2TM	Mit
Slc12a4	→	1.5	1.07	1.16	NP_033221	1085 AA., 12TM	Mit

Table 1: The putative targets from omics analysis, tissue expression pattern, and zebrafish screening. Summary of selected targets which highly expressed in heart and skeletal muscle from results of MS using mouse heart samples, Gene Chip analysis, quantitative analysis of mRNA expression in human tissues, and zebrafish screening. "Symbol" indicates the gene names. "Heart SR MS" showed the results of proteomics analysis in which arrows indicate the change of expression levels in TAC samples compared with normal samples and a minus sign indicates not detected. In GeneChip columns, the change of expression levels of diseased samples *vs.* normal samples are shown. NCBI accession numbers of genes (Mus musculus) are listed in the middle column. Amino acid length and transmembrane prediction: information on the amino acid length obtained from NCBI and the prediction of transmembrane helices from TMHMM (http://www.cbs.dtu.dk/services/TMHMM/) are indicated. Cellular localization shows the localization in the cell as predicted from NCBI information. ER: endoplasmic reticulum, Mit: mitochondria.

Figure 3: Quantitative analysis of *FITM* mRNA expression. Analysis of the mRNA expression in mouse tissues (a) and chambers of the human heart (b). Relative mRNA levels were quantified using the comparative ΔΔCT method with an internal control gene: *Ppia* for mouse tissues and *Ppia* for human cardiac organ. Expression levels relative to the expression levels of the heart and left atrium are shown. Placenta in the different chambers of the human heart graph was used as a control for the experiments. Each dot represents a replicate (n=2 or 3).

(Figure 6). This tendency for the levels of ER stress proteins to decrease was similar upon *FITM1*, *FITM2*, and *FITM1+FITM2* overexpression. In the heart, fatty acids are a preferable energy source and LDs are a universally conserved organelle that stores neutral lipids. We thus applied metabolomic analysis to investigate whether the promotion of LD formation or the existence of numerous LDs affects cellular metabolism. Although the levels of many metabolites changed upon transfection with a mock vector alone, *FITM1*- or *FITM2*-transfected and *FITM1+FITM2* co-transfected cells showed some characteristic changes compared with the mock-transfected cells. The changes included reduced total amino acid level, inactivation of the urea cycle, reduction of acylcarnitine (markedly in *FITM2*-transfected cells), and increased glucose-6-phosphate (especially in *FITM1*-transfected cells) (Figure 7). These results indicate that FITM proteins and lipid droplet formation influence ER function and induce metabolic changes.

Discussion

HF is a major cause of death and the number of HF patients continues to increase globally. This study explored novel drug targets for HF with a focus on SR/ER membrane. Proteome analysis of the mouse heart and liver identified 3,638 proteins from healthy SR/ER, TAC SR/ER, and liver ER proteins. In heart samples, we identified proteins expressed in SR, including SERCA2a, RyR2, Calumin, and TRIC-A. This indicated that proteomics could detect proteins expressed in heart SR and revealed the good quality of our dataset. In the transcriptome analysis, the genes up-regulated in heart failure included ANP and BNP, well known up-regulated proteins in heart failure. In addition, about 10% genes showed the changes of expression level, which is consistent to that relatively small number of proteins were regulated in TAC mice [42]. Collectively, our transcriptome

Figure 4: Involvement of FITM1 and FITM2 in lipid droplet formation. Constructs were transfected into HEK293 cells using Lipofectamine 2000 reagent. Cells were stained for lipid droplets using 1 μg/ml BODIPY 493/503 and visualized by EVOS FL (scale bar: 100 μm) and counted by In Cell Analyzer 1000. a: no transfection, b: pCMV6-entry (mock vector), c: *FITM1*, d: *FITM2*, e: *FITM1+FITM2*, f: area of lipid droplets, g: number of lipid droplets. Analysis was performed in 12 wells for each bar and data are represented as mean ± SD. The transfection (a-e) and droplet (f and g) experiments were replicated in twice with similar results.

dataset also suggested to be the good quality. Since sample sizes of our proteome and transcriptome analyses were very small, up- or down-regulation was not conclusive but indicative, and thus we chose genes for functional analysis based on not only omics data but also literatures and public database information. Finally, six genes were selected from the proteomic, genomic, and genetic approaches. We expected to find novel pharmaceutical targets capable of modulating cardiac cell function by control of ER/SR functions, such as ion channels and
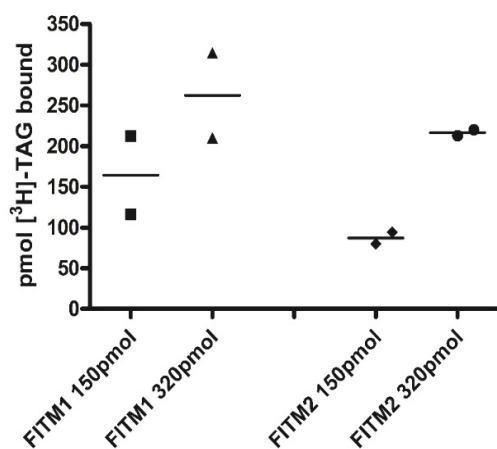
Figure 5: FITM1 and FITM2 binding to [9,10-3H(N)]-triolein. Recombinant proteins, [9,10-3H(N)]-triolein ([3H]-TAG), and Strep-tactin Macroprep beads were mixed by inversion for 4 h at room temperature. Beads were then measured for radioactivity using a scintillation counter. This experiment was repeated with similar results using three lots of recombinant proteins.
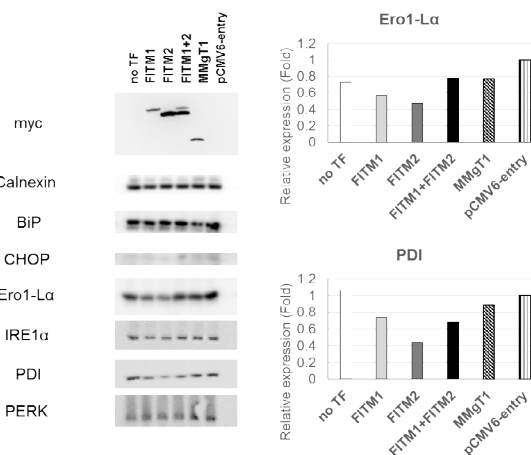

Figure 6: Effect of FITM overexpression on reducing the expression levels of ER stress marker proteins HEK293 cells were transiently transfected with mock, *FITM1*, *FITM2*, *FITM1+FITM2*, or *MMGT1*. Cells were lysed in Laemmli sample buffer and subjected to western blotting. Each sample was a pool of three wells. The graph at the right side of the blot shows quantification of Ero1-Lα and PDI protein levels after normalization to Calnexin and these levels are presented as the fold-change of the pCMV6 transfected sample. This experiment was reproduced twice with similar results.
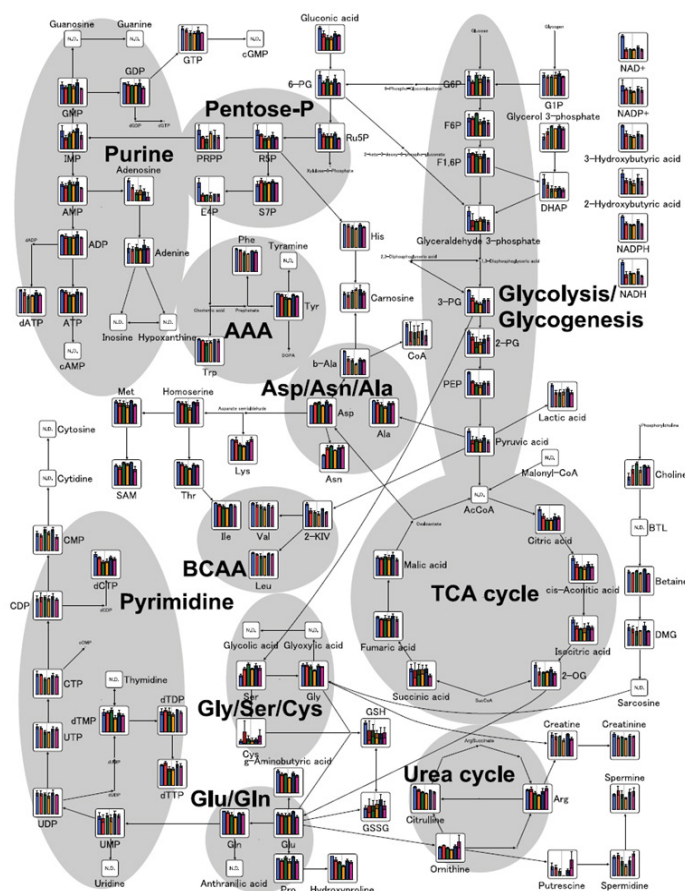

Figure 7: Metabolomic analysis of FITM-overexpressing cells. Mock, *FITM1*, *FITM2*, and *FITM1+FITM2* were transiently overexpressed in HEK293 cells. Cell lysates were subjected to CE-TOFMS and LC-TOFMS measurements. In each bar graph, the blue bars indicate the no transfection; red bars, pCMV6-entry (mock vector); green bars, FITM1; orange bars, FITM2; navy bars, FITM1+FITM2; and purple bars, other membrane protein.

transporter, and thus selected the membrane proteins with unknown functions in heart. We focused on members of a protein family associated with lipid droplet formation—FITM1 and FITM2— because *FITM1* and *FITM2* are highly expressed in the heart and skeletal muscles of mice and humans and since their biological function in the heart was unknown. Although we could not test statistical analysis in the analysis of mRNA expression because of limited sample availability, our data corresponded to the previous report [29]. Our overexpression assay using cultured cells indicated that *FITM1* and *FITM2* are involved in LD formation, ER function, and cellular metabolism. The overexpression of *FITM1*, *FITM2*, and *FITM1+FITM2* led to the accumulation of LDs, similar to the results described in a previous report [30]. In that report, there were no significant differences in the numbers of LDs between *FITM1*- and *FITM2*-overexpressing cells. However, we found that *FITM2* overexpression led to the accumulation of larger and more LDs than that of *FITM1*. We also found that recombinant FITM proteins showed a similar binding response to triglyceride in our experiments. If the differences in size and number of LDs are not due to the TG binding ability of this family of proteins, it may reflect their expression levels because FITM1 expression was lower than that of FITM2 in our double-overexpression experiment. Further studies are needed to examine the main cause of these differences in the number and size of LDs. Since ER stress response is activated in heart failure [10], we investigated the effects of *FITMs* on the ER stress response/UPR. The overexpression of *FITM1*, *FITM2*, or *FITM1+FITM2* led to decrease in the expression of Ero1 and PDI proteins. Ero1 and PDI are known to be involved in UPR. These proteins are up-regulated in the viable region of human ischemic hearts and have been reported as protective factors against ischemia *in vivo* and *in vitro* [27]. We showed the possible association between the ER stress response and FITM expression in HEK293 cells, suggesting that the up-regulation of FITM proteins is harmful to ER function. However, a definitive conclusion will require further analyses to examine their expression patterns and effects in cardiac cells and hearts *in vivo*. We found that *FITM* overexpression and changes in LD formation affect cellular metabolism. In a study on mice overexpressing skeletal muscle-specific *Fitm2* (CKF2), it was reported that medium- and long-chain acylcarnitine species were decreased and species of acylcarnitine with an odd number of C3 and C5:1 in the chain were increased [43]. These and other findings indicate that *Fitm2* overexpression leads to decreased fatty acid oxidation, increases the utilization of branched chain amino acids, enhances glucose uptake, and profoundly decreases cellular ATP levels in skeletal muscle. In our experiments with cultured cells, a decrease of total amino acids was observed. This may indicate that amino acid catabolism is reduced in cells overexpressing *FITM1*, *FITM2*, and *FITM1+FITM2*. A reduction of acylcarnitine (markedly in *FITM2*-transfected cells) and an increase of glucose-6-phosphate (especially in *FITM1*-transfected cells) were also observed. These findings suggest that abnormal β-oxidation and enhancement of glucose uptake or carbohydrate utilization occurred. In C2C12 cells overexpressing *FITM2*, the metabolic changes that occurred in CKF2 skeletal muscle were not recapitulated, but our experiments using HEK293 cells showed a response similar to that in CKF2 mice. FITM1 and FITM2 are involved in LD formation and affect the expression levels of UPR-related proteins and cellular metabolism *in vitro*. Considering that FITM1 and FITM2 are highly expressed in skeletal muscles and heart, the elucidation and modulation of their function may contribute to the development of drugs for cardiovascular disease by in turn modulating ER function and metabolism. In this study, we did not evaluate their function in healthy and diseased heart. We speculate that they have some roles in oxidative tissues by our *in*

vivo screening using zebrafish. Zebrafish with *Fitm1* knockdown or *Fitm1+Fitm2* double knockdown showed cardiovascular dysfunctions, while overexpression of the human mRNA of *FITM1* or *FITM2* also led to malformations. Therefore, it would be interesting to analyze their physiological roles in heart and heart failure at the whole body level. We are now analyzing the physiology of *Fitm1* or *FItm2* knockout mice. These experiments will provide useful information of FITM1 and FITM2 biological function in the heart.

References

1. Ponikowski P, Anker SD, Al Habib KF, Cowie MR, Force TL, et al. (2014) Heart failure: preventing disease and death worldwide. ESC Heart Fail 1: 4-25.

2. Shimokawa H, Miura M, Nochioka K, Sakata Y (2015) Heart failure as a general pandemic in Asia. Eur J Heart Fail 17: 884-892.

3. Harikrishnan S, Sanjay G, Anees T, Viswanathan S, Vijayaraghavan G, et al. (2015) Clinical presentation, management, in-hospital and 90-day outcomes of heart failure patients in Trivandrum, Kerala, India: the Trivandrum Heart Failure Registry. Eur J Heart Fail 17: 794-800.

4. Nguyen E, Weeda ER, White CM (2016) A review of new pharmacologic treatments for patients with chronic heart failure with reduced ejection fraction. J Clin Pharmacol 56: 936-947.

5. Metra M, Carubelli V, Ravera, A, Stewart, Coats AJ, et al. (2017) Heart failure 2016: still more questions than answers. Int J Cardiol 15: 766-777.

6. Xin M, Olson EN, Bassel-Duby R (2013) Mending broken hearts: cardiac development as a basis for adult heart regeneration and repair. Nat Rev Mol Cell Biol 14: 529-541.

7. Mesaeli N, Nakamura K, Opas M, Michalak M (2001) Endoplasmic reticulum in the heart, a forgotten organelle? Mol Cell Biochem 225: 1-6.

8. Michalak M, Opas M (2009) Endoplasmic and sarcoplasmic reticulum in the heart. Trends Cell Biol 19: 253-259.

9. Glembotski CC (2012) Roles for the sarco-/endoplasmic reticulum in cardiac myocyte contraction, protein synthesis, and protein quality control. Physiology 27: 343-350.

10. Doroudgar S, Glembotski CC (2012) New concepts of endoplasmic reticulum function in the heart: programmed to conserve. J Mol Cell Cardiol 55: 85-91.

11. Bers DM (2002) Cardiac excitation–contraction coupling. Nature 415: 198-205.

12. Sobie EA, Lederer WJ (2012) Dynamic local changes in sarcoplasmic reticulum calcium: physiological and pathophysiological roles. J Mol Cell Cardiol 52: 304-311.

13. Bers DM (2006) Altered cardiac myocyte Ca regulation in heart failure. Physiology 21: 380-387.

14. Louch WE, Sejersted OM, Swift F (2010) There goes the neighborhood: pathological alterations in T-tubule morphology and consequences for cardiomyocyte Ca^{2+} handling. J Biomed Biotechnol 2010: 1-17.

15. Sanderson JE (2007) Heart failure with a normal ejection fraction. Heart 93: 155-158.

16. Minamino T, Komuro I, Kitakaze M (2010) Endoplasmic reticulum stress as a therapeutic target in cardiovascular disease. Circ Res 107: 1071-1082.

17. Groenendyk J, Sreenivasaiah PK, Kim DH, Agellon LB, Michalak M, et al. (2010) Biology of endoplasmic reticulum stress in the heart. Circ Res 107: 1185-1197.

18. Anelli T, Sitia R (2008) Protein quality control in the early secretory pathway. EMBO J 27: 315-327.

19. Ron D, Walter P (2007) Signal integration in the endoplasmic reticulum unfolded protein response. Nat Rev Mol Cell Biol 8: 519-529.

20. Kim I, Xu W, Reed JC (2008) Cell death and endoplasmic reticulum stress: disease relevance and therapeutic opportunities. Nat Rev Drug Discov 7: 1013-1030.

21. Minamino T, Kitakaze M (2010) ER stress in cardiovascular disease. J Mol Cell Cardiol 48: 1105-1110.

22. Sawada T, Minamino T, Fu HY, Asai M, Okuda K, et al. (2010) X-box binding protein 1 regulates brain natriuretic peptide through a novel AP1/CRE-like element in cardiomyocytes. J Mol Cell Cardiol 48: 1280-1289.

23. Okada K, Minamino T, Tsukamoto Y, Liao Y, Tsukamoto O, et al. (2004) Prolonged endoplasmic reticulum stress in hypertrophic and failing heart after aortic constriction: possible contribution of endoplasmic reticulum stress to cardiac myocyte apoptosis. Circulation 110: 705-712.

24. Dally S, Monceau V, Corvazier E, Bredoux R, Raies A, et al. (2009) Compartmentalized expression of three novel sarco/endoplasmic reticulum Ca2ATPase 3 isoforms including the switch to ER stress, SERCA3f, in non-failing and failing human heart. Cell Calcium 45: 144-154.

25. Fu HY, Okada K, Liao Y, Tsukamoto O, Isomura T, et al. (2010) Ablation of C/EBP homologous protein attenuates ER-mediated apoptosis and cardiac dysfunction induced by pressure overload. Circulation 122: 361-369.

26. Thuerauf DJ, Marcinko M, Gude N, Rubio M, Sussman MA, et al. (2006) Activation of the unfolded protein response in infarcted mouse heart and hypoxic cultured cardiac myocytes. Circ Res 99: 275-282.

27. Severino A, Campioni M, Straino S, Salloum FN, Schmidt N, et al. (2007) Identification of protein disulfide isomerase as a cardiomyocyte survival factor in ischemic cardiomyopathy. J Am Coll Cardiol 50: 1029-1037.

28. Toko H, Takahashi H, Kayama Y, Okada S, Minamino T, et al. (2010) ATF6 is important under both pathological and physiological states in the heart. J Mol Cell Cardiol 49: 113-120.

29. Kadereit B, Kumar P, Wang WJ, Miranda D, Snapp EL, et al. (2008) Evolutionarily conserved gene family important for fat storage. Proc Natl Acad Sci USA 105: 94-99.

30. Gross DA, Zhan C, Silver DL (2011) Direct binding of triglyceride to fat storage-inducing transmembrane proteins 1 and 2 is important for lipid droplet formation. Proc Natl Acad Sci USA 108: 19581-19586.

31. Gross DA, Snapp EL, Silver DL (2010) Structural insights into triglyceride storage mediated by fat storage-inducing transmembrane (FIT) protein 2. PLoS One 5: e10796.

32. Rappsilber J, Mann M, Ishihama Y (2007) Protocol for micro-purification, enrichment, pre-fractionation and storage of peptides for proteomics using StageTips. Nat Protoc 2: 1896-1906.

33. Elias JE, Gygi SP (2007) Target-decoy search strategy for increased confidence in large-scale protein identifications by mass spectrometry. Nat Methods 4: 207-214.

34. Westerfield M (2000) The Zebrafish Book: A Guide for the Laboratory Use of Zebrafish (Danio rerio). University of Oregon Press, Eugene, OR.

35. Turner DL, Weintraub H (1994) Expression of achaete-scute homolog 3 in Xenopus embryos converts ectodermal cells to a neural fate. Genes Dev 8: 1434-1447.

36. Benjamini Y, Hochberg Y (1995) Controlling the false discovery rate: a practical and powerful approach to multiple testing. J R Stat Soc Series B Stat Methodol 57: 289-300.

37. Houser SR, Margulies KB, Murphy AM, Spinale FG, Francis GS, et al. (2012) Animal models of heart failure: a scientific statement from the American Heart Association. Circ Res 111: 131-150.

38. Dzieciatkowska M, Hill R, Hansen KC (2014) GeLC-MS/MS analysis of complex protein mixtures. Methods Mol Biol 1156: 53-66.

39. Zhang M, Yamazaki T, Yazawa M, Treves S, Nishi M, et al. (2007) Calumin, a novel Ca2+-binding transmembrane protein on the endoplasmic reticulum. Cell Calcium 42: 83-90.

40. Yazawa M, Ferrante C, Feng J, Mio K, Ogura T, et al. (2007) TRIC channels are essential for Ca2+ handling in intracellular stores. Nature 448: 78-82.

41. Choudhary V, Ojha N, Golden A, Prinz WA (2015) A conserved family of proteins facilitates nascent lipid droplet budding from the ER. J Cell Biol 211: 261-271.

42. Rüdebusch J, Benkner A, Poesch A, Dörr M, Völker U, et al. (2017) Dynamic adaptation of myocardial proteome during heart failure development. PLoS One 12: e0185915.

43. Miranda DA, Koves TR, Gross DA, Chadt A, Al-Hasani H, et al. (2011) Re-patterning of skeletal muscle energy metabolism by fat storage-inducing transmembrane protein 2. J Biol Chem 286: 42188-42199.